ORIGINAL PAPER

Micro-Raman study of copper hydroxychlorides and other corrosion products of bronze samples mimicking archaeological coins

Giulia Bertolotti · Danilo Bersani · Pier Paolo Lottici ·
Marcella Alesiani · Thomas Malcherek ·
Jochen Schlüter

Abstract Three bronze samples created by CNR-ISMN (National Research Council—Institute of Nanostructured Materials) to be similar to Punic and Roman coins found in Tharros (OR, Sardinia, Italy) were studied to identify the corrosion products on their surfaces and to evaluate the reliability of the reproduction process. Micro-Raman spectroscopy was chosen to investigate the corroded surfaces because it is a non-destructive technique, it has high spatial resolution, and it gives the opportunity to discriminate between polymorphs and to correlate colour and chemical composition. A significant amount of green copper hydroxychlorides ($Cu_2(OH)_3Cl$) was detected on all the coins. Their discrimination by Raman spectroscopy was challenging because the literature on the topic is currently confusing. Thus, it was necessary to determine the characteristic peaks of atacamite, clinoatacamite, and the recently discovered anatacamite by acquiring Raman spectra of comparable natural mineral samples. Clinoatacamite, with different degrees of order in its structure, was the major component identified on the three coins. The most widespread corrosion product, besides hydroxychlorides, was the red copper oxide cuprite (Cu_2O). Other corrosion products of the elements of the alloy (laurionite, plumbonacrite, zinc carbonate) and those resulting from burial in the soil (anatase, calcite, hematite) were also found. This study shows that identification of corrosion products, including discrimination of copper hydroxychlorides, could be accomplished by micro-Raman on valuable objects, for example archaeological findings or works of art, avoiding any damage because of extraction of samples or the use of a destructive analytical technique.

Keywords Raman spectroscopy · Copper hydroxychlorides · Coins · Bronze · Corrosion products · Archaeological metals

G. Bertolotti (✉) · D. Bersani · P. P. Lottici
Dipartimento di Fisica, University of Parma,
Viale G.P. Usberti 7/a,
43100 Parma, Italy
e-mail: giulia.bertolotti@ing.unitn.it

M. Alesiani
Dipartimento di Energetica, University of Rome "La Sapienza",
Via A. Scarpa 16,
00161 Rome, Italy

T. Malcherek · J. Schlüter
Mineralogisches Museum, Universität Hamburg,
Grindelallee 48,
20146 Hamburg, Germany

Introduction

The characterization of corrosion products on metallic archaeological artefacts is the starting point in the development of suitable conservation treatments that enable preservation of the objects and the information they carry long into the future. Thus, it is important to develop accurate methods of analysis that exploit each technique to the utmost. Considering that archaeological finds are unique and should not be damaged, it is recommended to produce within the laboratory comparison samples as similar as possible to the real materials, to be used to test and implement the analytical procedures. The CNR-ISMN (National Research Council—Institute of Nanostructured Materials) attempted to imitate some Punic and Roman

bronze coins found at the archaeological site of Tharros (OR, Sardinia, Italy) both in their base alloy and in the corrosion patterns on their surfaces. In the laboratory, different coin-shaped base alloys were produced, and chemically attacked with acids to develop the most common decay pattern made up mainly by reddish copper oxides and green hydroxychlorides. Some of the samples were also buried in Tharros to trigger the development of more complex compounds because of interaction of the metal surface with soil. Micro-Raman spectroscopy was used in this study to confirm that the different reproduction processes of the corrosion patterns led to the development of different compounds on the surfaces of the samples. This analytical technique was chosen after an in depth investigation of the literature on corrosion studies in the field of cultural heritage science, because many researchers [1–4, 8–10, 19, 20, 22] have already emphasized how Raman spectroscopy guarantees high resolution, non-destructiveness, correlation between appearance and chemical composition, discrimination of polymorphs, and identification of the spatial distribution of corrosion products. The spread of awareness in the scientific community of these benefits could help to enlarge the databases of spectra of corrosion products required for the identification of a phase encountered on a corroded artefact. The current literature on the discrimination of copper hydroxychlorides, chemical formula $Cu_2(OH)_3Cl$, by Raman spectroscopy is not clear, because of the finding of new mineral species with different crystal structures belonging to this group that has every time questioned previous studies [13] and the publication of different Raman spectra for the same mineralogical species [6, 9]. Comparison of spectra of paratacamite available in the literature is, perhaps, the most evident proof of the existing uncertainty among the data. For instance, the published data provided by the RRUFF database [6] and Frost [9] are, in fact, quite different. Paratacamite has the chemical formula $(Cu, M)_2(OH)_3Cl$ where M is defined as either zinc or nickel, and whose structure was structurally defined by Fleet [7] as having a space group R-3. A substructure of paratacamite (space group R-3 m) was eventually equated with paratacamite, and it is unclear whether paratacamite with space group R-3 actually exists. It is usually accepted that substantial amounts of Zn (or Ni) are required to stabilize this substructure, thus paratacamite cannot be regarded as a polymorph of atacamite. Today the name paratacamite is often used for mixed crystals, and some authors prefer to regard it as Cu-enriched herbertsmithite ($Cu_3Zn(OH)_6Cl_2$). Nevertheless, many crystallographic databases, in particular that related with X-ray diffraction, are still using the term "paratacamite", even for clinoatacamite (defined sometimes as "monoclinic paratacamite"). Being a solid

solution or a mixture of different phases there might be infinite numbers of different chemical compositions that would give different Raman spectra and thus we decided to exclude this hydroxychloride from our study as a comparison sample cannot be defined. Characterization and comparison of the phases of the $Cu_2(OH)_3Cl$ group is of great importance considering that copper hydroxychlorides are studied in other fields of cultural heritage science and in other research areas of materials science in general. Some copper hydroxychlorides, in fact, were used as pigments or have been detected as impurities or decay products of other pigments [3]. They are, moreover, also found as corrosion products on archaeological glass windows [3]. Atacamite was detected in the jaws of the marine worm *Glycera dibranchiata* [14] forming with proteins a biomineral structure which could inspire the production of synthetic new biomaterials characterized by lightness and high resistance to abrasion [15]. Finally, magnetic properties of this group of minerals are of interest, considering their copper and oxygen content which bears comparison with superconducting cuprates with high Tc [21, 23]. In all these fields the availability of a database of spectra could be useful.

This research was conducted in two stages. First a set of comparison samples of copper hydroxychlorides was analysed in order to identify the discriminating features of their Raman spectra. Second, the spectra measured on the reproduced coins were compared with those in the database built in the first stage and in other available databases and published literature.

Materials and methods

The copper hydroxychloride comparison samples

To build a database of comparison spectra of copper hydroxychlorides three samples were selected as reference for the polymorphs—atacamite, clinoatacamite, and anatacamite (Fig. 1). Botallackite, another monoclinic polymorph of atacamite, was not considered in this study because it is the most unstable of the minerals of the group and, thus, it is not commonly detected as corrosion product.

Atacamite is the most naturally abundant polymorph of pure $Cu_2(OH)_3Cl$. It crystallizes in the orthorhombic system and space group Pnam. The atacamite sample is a crystal from Atacama, Chile. Under the optical microscope it is prismatic and bright green in colour with a vitreous lustre.

Clinoatacamite is monoclinic with class 2/m and space group P2$_1$/n. It is biaxial negative and was defined in 1996 by Jambor et al. [13]. The sample analyzed in this study was characterized by energy dispersive X-ray analysis
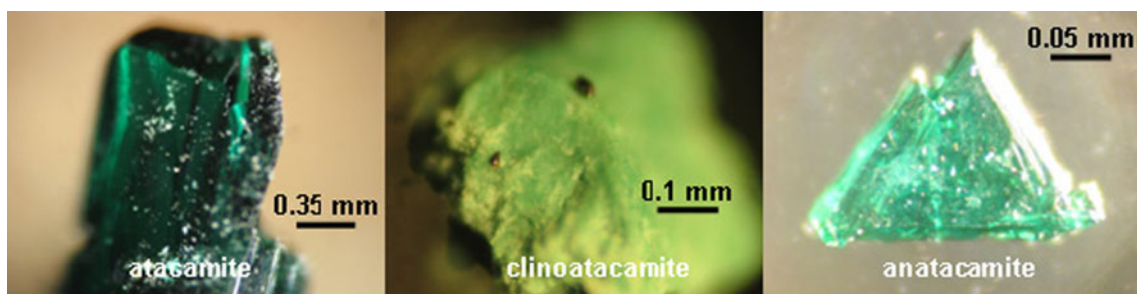
Fig. 1 Stereomicroscope images of the samples used as comparison to build the database of Raman spectra of copper hydroxychlorides

(EDX), X-ray photoelectron spectroscopy (XPS), and infrared spectroscopy (IRS) by Hayez [10].

A triangular crystal of the recently discovered phase anatacamite was provided by the Mineralogisches Museum of the University of Hamburg (Germany), that first identified and characterized the mineral by XRD [18]. This mineral is triclinic with space group $P\bar{1}$ and strong trigonal pseudo-symmetry. Its structure is a distorted version of the ordered paratacamite structure (SG R-3) described by Fleet (1975) [7].

The bronze samples

The three samples studied in this research were created by CNR-ISMN (National Research Council—Institute of Nanostructured Materials) as a part of the EFESTUS project financed by the European Commission in the period 2003–2005. They are part of a larger group of samples which mimic Punic and Roman coins found in the archaeological site of Tharros (OR, Sardinia, Italy) both in their chemical composition and in their metallurgical characteristics. The three circular samples used in this study weigh approximately 12–15 g and have a diameter of 2.5–3 cm. Their composition is given in Table 1.

The base copper alloys underwent tailored accelerated decay which consisted in chemically induced degradation followed by artificial aging. Details of the production and treatment of the whole group of samples created by CNR-ISMN are given in a related publication

[5]. In particular, the THT128-Tumore sample was treated to exhibit bronze disease features. THT128, instead, was buried for two years in Tharros after the chemical treatments to induce the production of complex corrosion products on its surface by interaction with soil components. Pictures of the three samples after the artificial decay are given in Fig. 2. Many analyses were conducted by CNR-ISMN itself on these samples and their results have already been published [11, 12].
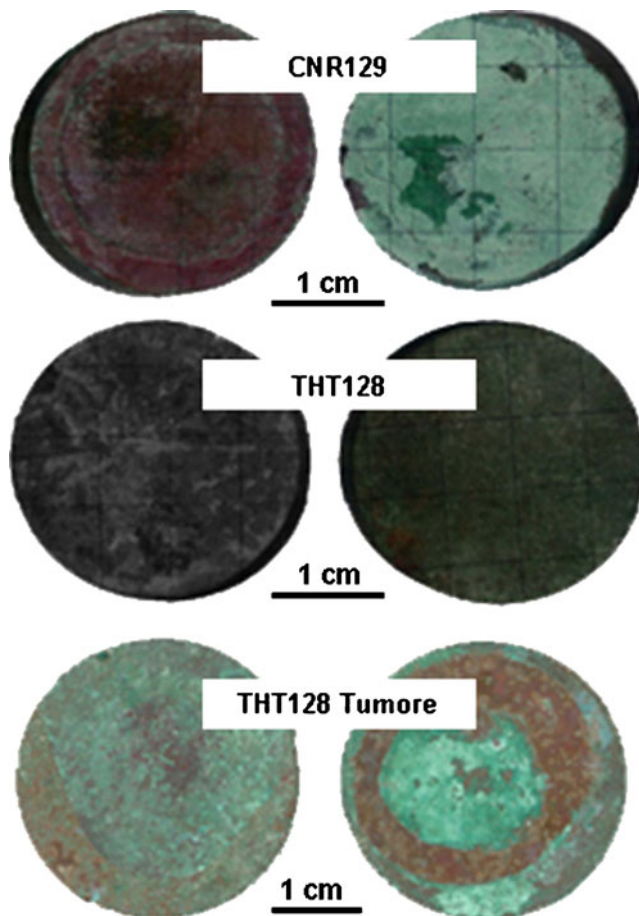

Fig. 2 Images of the bronze samples mimicking ancient coins. For each coin the pictures of the two sides are given side by side

Table 1 Composition (% w/w) of the bronze samples mimicking ancient coins

	CNR 129 (quaternari bronze)	THT128 Tumore and THT128 (lead bronze)
Cu	82.3	92.3
Sn	3.0	7.5
Pb	0.5	0.2
Zn	14.0	–
Sulfides	Inclusions	Inclusions

Instruments

Micro-Raman measurements were performed at the Physics Department of the University of Parma with a Jobin–Yvon Horiba LabRam spectrometer, equipped with holographic notch filter, motorized x–y stage, auto-focus, and an Olympus BX40 microscope with objectives up to 100×. The light at 632.8 nm of a He/Ne laser (maximum power 30 mW) was used for excitation. Neutral density filters, generally D0.6, were used to keep the laser power at a low level (0.05–1 mW) on the samples, to avoid laser-induced transformations. The spectra were collected using 50× and 100× objectives with repeated acquisition (2 to 4, according to the signal-to-noise ratio) of 30–60 s. Calibration of the spectrometer was checked by using the 520.6 cm^{-1} line of a silicon wafer. The laser spot diameter was ~1 μm.

Data collection and analysis

Copper hydroxychlorides comparison sample

Raman measurements were acquired on the atacamite crystal with the polarization of the laser beam oriented at 0°, 45°, and 90° with respect to the c axis to check the variation of the relative intensities of the Raman bands with orientation.

On the anatacamite sample the spectra were measured along two mutually orthogonal orientations, suggested by the morphology of the crystal.

Bronze samples mimicking ancient coins

On the surface of the coins measurements were collected from visually different points. To identify an unknown spectrum, comparisons were made with reference on-line databases, the literature, and the previously acquired set of comparison spectra of copper hydroxychlorides.

Results and discussion

Copper hydroxychlorides comparison samples

The Raman spectra of the three copper hydroxychlorides considered in this study are different and thus distinguishable even by simple visual comparison (Figs. 3 and 4). The Raman shifts for the three comparison samples are listed in Table 2. The Raman spectra of basic copper chlorides are usually divided into three regions. At high wavenumbers, between 3300 and 3450 cm^{-1}, the OH stretching vibrations are present [8, 16]. The number of peaks in this region usually reflects the number of different OH groups present in the structure, except in the case of strong overlap of the bands. The region
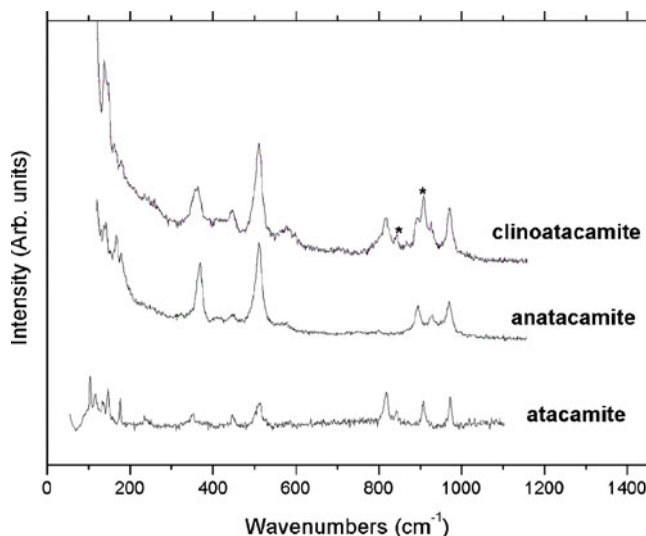

Fig. 3 Raman spectra of the three reference samples in the region around 600 cm^{-1}. The *asterisks* identify the peaks from atacamite in the spectra of other polymorphs

between 800 and 1000 cm^{-1} is usually assigned to OH-deformation modes, but recent work by Liu et al. [16] shows how those bands should be better related to Cu–O–H bending modes—this would also explain the different number of OH stretching bands. Finally, the region at wavenumbers below 600 cm^{-1} includes O–Cu–O and Cl–Cu–Cl bending vibrations and lattice modes. While the main peak near 500 cm^{-1} is usually attributed to O–Cu–O symmetric stretching, assignment of the other bands is still debated [8, 16].

In general, copper hydroxychlorides can be distinguished from other corrosion products in the medium-frequency region of the Raman spectrum. Common features of the analyzed compounds are a peak around 511 cm^{-1} and
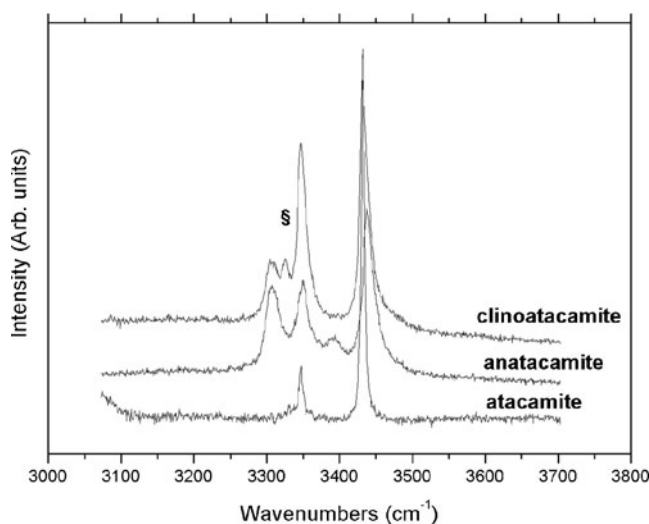

Fig. 4 Raman spectra of the three reference samples in the region around 3400 cm^{-1}. The symbol § identifies a peak which might not be from clinoatacamite

Table 2 Raman shifts measured on the three comparison samples, in wavenumbers (cm^{-1})

	Atacamite	Clinoatacamite	Anatacamite
O–Cu–O and Cl–Cu–Cl stretching and bending, lattice modes	105		
	117		
			126
	135	139	
	148		143
			166
	177		
	353	361	367
			412
			420
		446	446
	513	511	510
	587	581	579
Hydroxyl deformation			747
	819	818	800
	846		
		893	896
	909		
		927	930
	975	971	971
Hydroxyl stretching		3308	3310
		3326	
	3348	3348	3350
			3393
	3433	3434	3439

at least three peaks between 780 and 1000 cm^{-1}. A flow-chart to identify some copper hydroxychlorides by Raman (Fig. 5) was developed in this study after observing and comparing, region by region, all the acquired spectra.
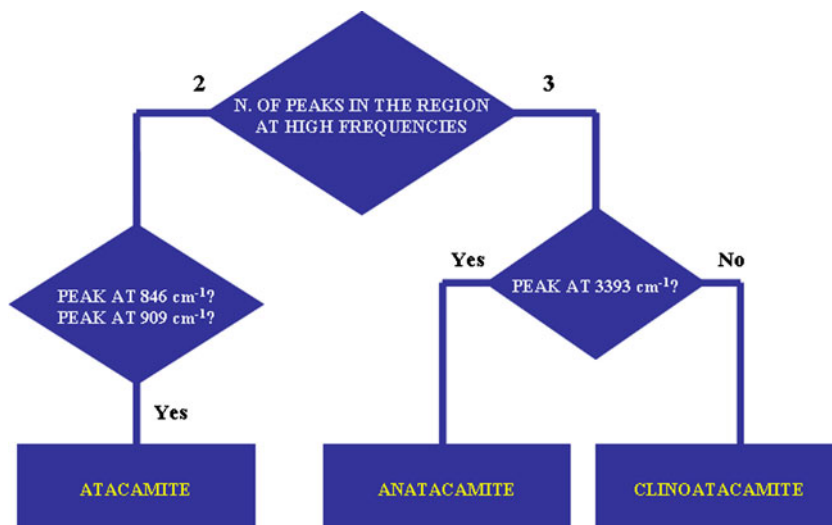
The measured atacamite spectrum is similar to those published by Bouchard [3, 4], in the RRUFF database [7], and published by Frost for an Australian sample [8]. On rotating the crystal, changes in the intensities of the peaks are evident. The highest similarity with data available in the literature is observed when the laser polarization is at 45° with respect to c axis. In the low–medium wavenumber region the spectrum of atacamite has a peak at lower wavenumber (353 cm^{-1}) than the other hydroxychlorides (ca 364 cm^{-1}) and two characteristic peaks at 846 and 909 cm^{-1}.

The Raman spectrum acquired from the comparison sample for the phase clinoatacamite shows that it also contains the phase atacamite. After the subtraction of the atacamite spectrum, a spectrum similar to those published by Hayez [10] and Liu et al. [16] for pure clinoatacamite is obtained. The band at 3326 cm^{-1} (Fig. 4), even if present in many spectra, does not seems characteristic of clinoatacamite and might arise from an undetermined minor phase. Not considering this band as due to clinoatacamite, there are only three OH-stretching peaks, as would be expected considering that there are only three crystallographically inequivalent OH groups in its structure.

Because of the very recent discovery of anatacamite [17, 18] (2009), to the author's knowledge no Raman spectra have been reported in the literature for this phase, except the one shown in the RRUFF database [7]. Very good correspondence is found between the spectra reported by RRUFF and that obtained in this work, except for an extra peak at 913 cm^{-1} present in the RRUFF spectrum.

A peak at 894 ca cm^{-1} enables discrimination of clinoatacamite and anatacamite from atacamite. Discrimination between clinoatacamite and anatacamite is challenging by X-ray powder diffraction experiments [17] and also by use of the Raman technique if only the medium-

Fig. 5 Diagram representing the process for the discrimination of the copper hydroxychlorides atacamite, clinoatacamite, and anatacamite by their Raman spectrum

wavenumber region of the spectrum is considered. However, observation of the high-wavenumber region enables one to recognize anatacamite from the presence of a weak peak at 3393 cm^{-1} (Fig. 4). Therefore, a total of four OH-stretching peaks is observed in the anatacamite spectrum. The mineral has twelve different OH groups in its structure, but its strong pseudo-symmetry might explain why it gives rise to four OH bands only, with the signals from three positions overlapping for each.

Bronze samples mimicking ancient coins

On the surface of the samples mimicking ancient coins many compounds have been detected, as is shown in Table 3.

On all the coins a significant amount of green copper hydroxychlorides was found. A specific area on the surface of the green side of sample CNR129 was chosen for in-depth investigation because of its very heterogeneous appearance under microscope observation—different hues of green and different crystalline features were present. Raman measurements revealed a direct correlation between appearance (in terms of colour and shapes) and composition. The most dark and crystalline area was identified as clinoatacamite. The spectrum of the light green zone, without well defined crystalline shapes, gave poorly defined peaks between 850 and 1000 cm^{-1}, broader than in the clinoatacamite spectrum (Fig. 3). In addition, all the measured Raman peaks were red-shifted compared with the clinoatacamite peaks. We can exclude a thermal origin for the broadening and the red-shift of the spectral features, because strong variations in the laser power did not produce any visible effect in the spectra. This area has holes paved with a sea-green amorphous-like material that, when analysed by micro-Raman spectroscopy, was characterized by even more undefined and broad peaks.

The green patina present on sample THT128 had only the sharp Raman features of clinoatacamite, whereas sample THT128-Tumore was characterized by the presence of different hydroxychlorides. The most widespread was, in this case also, clinoatacamite, but in some areas the more disordered copper hydroxychloride detected on sample CNR129 was found, and a small amount of atacamite (usually mixed with clinoatacamite).

The most widespread corrosion product, besides hydroxychlorides, was the red copper oxide cuprite (Cu_2O); a layer of octahedral cuprite crystals was usually detected under the green patinas. Because of the high spatial resolution of Raman spectroscopy, the spectra of some minor phases were also acquired (Table 3). Among these, many, for example laurionite, plumbonacrite, and zinc carbonate, came from transformation of the alloying elements. The high Raman signal of many lead compounds made them easily detectable even if lead was present in small amounts. Other compounds found in the THT128 coin, for example calcite and anatase, come from the soil and adhered to the surface of sample THT128 during burial.

Conclusions

This study confirmed that micro-Raman spectroscopy is an excellent technique for discrimination of polymorphs and which enables recognition of differences between the spectra of the green corrosion products with chemical formula $Cu_2(OH)_3Cl$, although they are often present together both in natural and artificial samples. The need emerged for measurements with an extended range of wavenumbers including the regions of both hydroxyl stretching (approx. 3400 cm^{-1}) and deformation (700–990 cm^{-1}). Atacamite can be identified by the presence of

Table 3 Corrosion products detected on the bronze samples imitating ancient coins by micro-Raman spectroscopy

Name	Chemical formula	Colour	CNR129	THT128 Tumore	THT128
Anatase	TiO$_2$	Pink, silver light blue			X
Calcite	CaCO$_3$	Grey, pink, yellow, light blue/green/yellow patina adherent to the metal bulk		X	X
Clinoatacamite	Cu$_2$(OH)$_3$Cl	Green	X	X	X
Cuprite	Cu$_2$O	Pink or red	X	X	
Ematite	Fe$_2$O$_3$	Pink or yellow	X		X
Laurionite	PbClOH	White	X		
Lead carbonate		White or grey	X	X	
Paratacamite	Cu$_2$(OH)$_3$Cl	Green	X	X	
Plumbonacrite	Pb$_5$O(OH)$_2$(CO$_3$)$_3$	Greenish silver grey	X		
Sulfides		Black or blue	X		X
Tenorite	CuO	Bronze	X		
Zinc carbonate		Brownish red	X		

peaks at 846 cm^{-1}, 909 cm^{-1}, two peaks in the hydroxyl-stretching region, and a peak around 353 cm^{-1}, which in the other phases is found at higher wavenumbers. Clinoatacamite has a spectrum very similar to tat of anatacamite but this latter phase gives a characteristic peak at 3393 cm^{-1}. This study serves to establish that identification of copper hydroxychlorides can be accomplished without destructive testing of samples. This is a key point for a technique to be used in the analysis of archaeological findings or works of art, where non-invasive testing procedures are desirable. It is still unknown whether the recently discovered phase anatacamite exists as corrosion product. Considering that it is formed from a very pure copper hydroxychloride solution, that a small presence of zinc ions tends to stabilize clinoatacamite [13], and higher amounts of impurities would lead to the formation of "paratacamite" [17], it is unlikely that anatacamite would be found as corrosion product on bronze objects, although we hypothesize that it could be detected on copper artefacts. Publication of the Raman spectra (Figs. 3 and 4) obtained in this study will hopefully become a helpful tool for future analysis of archaeological samples.

The high spatial resolution of micro-Raman spectroscopy enabled characterization of the corrosion patina of bronze objects on a microscopic scale. Green compounds on bronze samples mimicking ancient coins were found to contain, primarily, clinoatacamite with different degrees of order. Minor corrosion products, involving alloying elements, for example lead and zinc, were also identified. However, it is possible that some sulfates and sulfides, with low Raman signal, were not detected. Hence, further analysis with complementary techniques should be conducted for complete characterization of the patinas.

With regard to the purpose of evaluating the reproduction process conducted by CNR-ISMN it can be said that the period of burial after chemical treatment experienced by the sample THT128 guaranteed more reliable simulation of archaeological findings because of the detection of soil components on the metal surface.

References

1. Bernard MC, Joiret S (2009) Understanding corrosion of ancient metals for the conservation of cultural heritage. Electrochimica Acta: 5199–5205
2. Bouchard M, Smith DC (2001) Evaluating Raman Microscopy for the non-destructive archaeometry of corroded coins: a powerful technique for conservation studies. Asian Chem Lett 5(3):157–170
3. Bouchard-Abouchacra M (2001) Evaluation des Capacités de la Microscopie Raman dans la Caractérisation Minéralogique et Physico-chimique de Matériaux Archéologiques: Métaux, Vitraux & Pigments, Paris. Museum National d'Histoire Naturelle
4. Bouchard M, Smith DC (2003) Catalogue of 45 reference Raman spectra of minerals concerning research in art history or archaeology, especially on corroded metals and coloured glass. Spectrochim Acta Part A 59:2247–2266
5. Casaletto MP, De Caro T, Ingo GM, Riccucci C (2006) Production of reference "ancient" Cu-based alloys and their accelerated degradation methods. Appl Phys A 83:617–622
6. Downs R T (2006) The RRUFF Project: an integrated study of the chemistry, crystallography, Raman and infrared spectroscopy of minerals. Program and Abstracts of the 19th General Meeting of the International Mineralogical Association in Kobe, Japan. O03-13
7. Fleet ME (1975) The crystal structure of paratacamite, Cu$_2$(OH)$_3$Cl. Acta Crystallogr B31:183–187
8. Frost RL, Martens W, Kloprogge JT, William PA (2002) Raman spectroscopy of the basic copper chloride minerals atacamite and paratacamite – implications for the study of copper, brass and bronze objects of archaeological significance. J Raman Spectrosc 33(10):801–806
9. Frost RL (2003) Raman spectroscopy of selected copper minerals of significance in corrosion. Spectrochim Acta Part A 59:1195–1204
10. Hayez V (2005/2006) Use of micro-Raman spectroscopy for the study of the atmospheric corrosion of copper alloys of cultural heritage. PhD Theses at Vrije Universiteit Brussel, Belgium
11. Ingo GM, De Caro T, Riccucci C, Angelini E (2006) Large scale investigation of chemical composition, structure and corrosion mechanism of bronze archaeological artefacts from Mediterranean basin. Appl Phys A 83:513–520
12. Ingo GM, De Caro T, Riccucci C, Khosroff S (2006) Uncommon corrosion phenomena of archaeological bronze alloys. Appl Phys A 83:581–588
13. Jambor JL, Dutrizac JE, Roberts AC, Grice JD, Szymanski JT (1996) Clinoatacamite, a new polymorph of Cu$_2$(OH)$_3$Cl, and its relationship to paratacamite and "anarakite". Can Mineral 34:61–72
14. Lichtenegger HC, Birkedal H, Casa DM, Cross JO, Heald SM, Waite JH, Stucky GD (2005) Distribution and role of trace transition metals in Glycera worm jaws studied with synchrotron microbeam techniques. Chem Mater 17:2927–2931
15. Lichtenegger HC, Schöberl T, Bartl MH, Waite H, Stucky GD (2002) High abrasion resistance with sparse mineralization: copper biomineral in worm jaws. Science 298:389–392
16. Liu X, Meng D, Zheng X, Hagihala M, Guo Q (2011) Mid-IR and raman spectral properties of clinoatacamite-structure basic copper chlorides. Adv Mater Res 146–147:1202–1205
17. Malcherek T, Schlüter J (2010) Anatacamite from La Vendida mine, Sierra Gorda, Atacama desert, Chile: a triclinic polymorph of Cu$_2$(OH)$_3$Cl. N. Jb. Miner Abh 187/3:307–312
18. Malcherek T, Schlüter J (2009) Structures of the pseudo-trigonal polymorphs of Cu$_2$(OH)$_3$Cl. Acta Crystallogr B65:334–341
19. Orlić N, Jelovica I, Dobrinić J, Lofrumento C, Salvi PR (2007) Analysis of ancient and medieval specimens using nondestructive spectroscopic techniques. Nucl Instrum Methods Phys Res A 580:739–742
20. Quaranta M, Sandu I (2008) Micro-stratigraphy of copper-based archaeological objects: description of degradation mechanisms by means of an integrated approach. 9th International Conference on NDT of Art, Jerusalem, Israel, 25–30 May 2008
21. Wills AS, Henry J-Y (2008) On the crystal and magnetic ordering structures of clinoatacamite, γ-Cu$_2$(OD)$_3$Cl, a proposed valence bond solid. J Phy Condens Matter 20:1–8
22. Young ML, Casadio F, Marvin J, Chase WT, Dunand DC (2010) An ancient Chinese bronze fragment re-examined after 50 years: contributions from modern and traditional techniques. Archaeometry
23. Zheng XG, Otabe ES (2004) Antiferromagnetic transition in atacamite Cu$_2$Cl(OH)$_3$. Solid State Commun 130:107–109